PHYSICAL REVIEW E **68**, 031706 (2003)

High-resolution x-ray study of the nematic–smectic-*A* and smectic-*A*–smectic-*C* transitions in liquid-crystal–aerosil gels

P. S. Clegg and R. J. Birgeneau
Department of Physics, University of Toronto, Toronto, Ontario, Canada M5S 1A7

S. Park* and C. W. Garland
Center for Material Science and Engineering, Massachusetts Institute of Technology, Cambridge, Massachusetts 02139, USA

G. S. Iannacchione
Department of Physics, Worcester Polytechnic Institute, Worcester, Massachusetts 01609, USA

R. L. Leheny
Department of Physics and Astronomy, Johns Hopkins University, Baltimore, Maryland 21218-2686, USA

M. E. Neubert
Liquid Crystal Institute, Kent State University, Kent, Ohio 44242, USA

(Received 14 May 2003; published 19 September 2003)

The effects of dispersed aerosil nanoparticles on two of the phase transitions of the thermotropic liquid-crystal material 4-*n*-pentylphenylthiol-4′-*n*-octyloxybenzoate ($\bar{8}S5$) have been studied using high-resolution x-ray diffraction techniques. The aerosils hydrogen bond together to form a gel which imposes a weak quenched disorder on the liquid crystal. The smectic-*A* fluctuations are well characterized by a two-component line shape representing thermal and random-field contributions. An elaboration on this line shape is required to describe the fluctuations in the smectic-*C* phase; specifically the effect of the tilt on the wave-vector dependence of the thermal fluctuations must be explicitly taken into account. Both the magnitude and the temperature dependence of the smectic-*C* tilt order parameter are observed to be unaffected by the disorder. This may be a consequence of the large bare smectic correlation length in the direction of modulation for this transition. These results show that the understanding developed for the nematic to smectic-*A* transition for octylcyanobiphenyl and octyloxycyanobiphenyl liquid crystals with quenched disorder can be extended to quite different materials and transitions.

DOI: 10.1103/PhysRevE.68.031706 PACS number(s): 64.70.Md, 61.30.Eb, 61.10.−i

I. INTRODUCTION

The phase transition behavior of many thermotropic liquid crystals (LCs) is quite well characterized [1] making liquid crystals ideal materials for studying the effects of weak perturbations, including especially quenched random fields and interactions. In a recent series of papers [2–5], it has been shown that the nematic to smectic-*A* (*N*-Sm*A*) transition in liquid crystal–aerosil dispersions is well described as a continuous symmetry (*XY*) transition with quenched random fields. This facilitates studying this important class of transitions. Early calorimetric studies have shown a systematic variation in the critical fluctuations as the aerosil concentration increases. These experiments and accompanying theory have focused on the isotropic to nematic (*I*-*N*) [6] and the *N*-Sm*A* transitions [2–6]. Here we present results on a substantially different material at the *N*-Sm*A* transition and we present x-ray data for the smectic-*A* to smectic-*C* (Sm*A*-Sm*C*) transition for liquid-crystal–aerosil dispersions. The Sm*A*-Sm*C* transition for heptyloxybenzylidene (7O.4)-aerosil dispersions has previously been investigated using ac calorimetry [7].

4-*n*-pentylphenylthiol-4′-*n*-octyloxybenzoate ($\bar{8}S5$) is a nonpolar liquid crystal with a succession of ordered phases (Fig. 1). At $T_{NA}^0 = 336.6$ K a transition from the orientationally ordered *N* phase to the layered Sm*A* phase occurs. For this particular liquid crystal the pretransitional correlation volume is highly anisotropic [10]. As we shall demonstrate in the present work, this gives rise to a strong asymmetry in the powder-averaged line shape observed with x-ray diffraction. This effect is enhanced by the relatively small fourth-order correction to the correlation function in the transverse

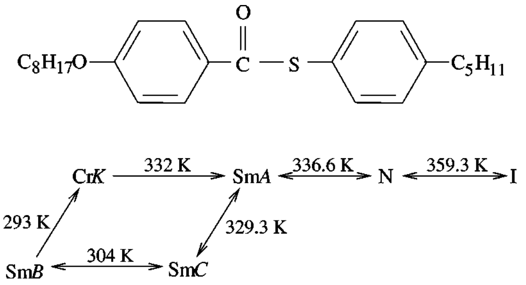

FIG. 1. The chemical structure and phase sequence for bulk $\bar{8}S5$. The transition temperatures are those given in Refs. [8,9].

---

*Present address: Center for Neutron Research, National Institute of Standards and Technology, Gaithersburg, MD 20899, USA.

1063-651X/2003/68(3)/031706(7)/$20.00

direction. Thus, the spherically averaged smectic line shape is very different from that observed for materials such as octylcyanobiphenyl (8CB) and octyloxycyanobiphenyl (8OCB). Consequently, this $\bar{8}S5$ study provides a test of the generality of the line-shape analysis used in Refs. [3,5] versus that used in Ref. [11]. As the temperature is lowered further, $\bar{8}S5$ exhibits a Sm*A*-Sm*C* transition ($T_{AC}^0 = 329.3$ K) where the molecules develop a tilt with respect to the layer normal. The tilt angle is the order parameter for this phase transition. The transitional behavior has mean-field rather than critical characteristics albeit with an anomalously large sixth-order term in the free energy [12,13], which is typical for the Landau tricritical to mean-field crossovers observed for most Sm*A*-Sm*C* transitions [14].

A liquid crystal is perturbed with weak-to-intermediate strength quenched disorder when aerosil particles are introduced. These particles are ∼7 nm diameter silica spheres with hydrophilic surfaces. When aerosil is dispersed in a liquid crystal, hydrogen bonds are formed between the aerosil particles creating a low density gel. On very long length scales the gel structure exhibits fractal correlations [6]; however, the gel has no particular correlations commensurate with the wave vector of the Sm*A* structure and hence is effectively random for our purposes. Here we present high-resolution x-ray diffraction measurements for $\bar{8}S5$ samples containing a range of concentrations of aerosil particles. Both the Sm*A*-type and Sm*C*-type liquid-crystal correlations in these samples have been characterized as a function of temperature.

Previous x-ray studies of the *N*-Sm*A* transition in liquid-crystal–aerosil dispersions demonstrated that the transition responded to the aerosil as though its principal effect was to apply a random field that pinned the phase of the density wave [2,3,5]. The static random-field fluctuations are more effective than thermal fluctuations at destroying long-range smectic order and this was evident in the development of the structure factor as a function of temperature and aerosil concentration. Here we wish to investigate whether the nonpolar $\bar{8}S5$ is less strongly perturbed than the polar cyano materials 8CB and 8OCB were. In addition, the tilt order parameter at the mean-field Sm*A*-Sm*C* transition couples to the aerosil in a different manner than the Sm*A* order parameter.

Section II describes the experimental techniques used to make and study the samples. In Sec. III the analysis protocol is outlined and the data and model parameters are presented. Finally in Sec. IV we draw conclusions from our measurements.

II. EXPERIMENTAL TECHNIQUES

The $\bar{8}S5$ was synthesized at Kent State University and the transition temperatures were observed to be close to those previously recorded for the bulk material [8,9]. The aerosil particles (hydrophilic type-300) were provided by Degussa and were dried prior to sample preparation. The aerosil concentration was characterized by ρ_S, the mass of aerosil divided by the volume of liquid crystal. Samples with $\rho_S = 0.0$, 0.025, 0.039, 0.073, 0.096, 0.220, and 0.350 g cm^{-3} were prepared (we drop the units hereafter). The corresponding pore volume fractions and mean pore sizes are given in Table I. As with previous studies of 8OCB-aerosil dispersions [5], it was necessary to avoid crystallization of the $\bar{8}S5$ samples prior to measurement since this results in phase separation. The aerosil particles were dispersed in a solution of $\bar{8}S5$ in spectroscopic grade acetone; the system was then sonicated and kept well above the crystallization temperature until the measurements were performed. The x-ray studies were undertaken once the acetone solvent had been evaporated. The sample environment and experimental geometry have been described in detail previously [5]. The studies were made using 8 keV x-rays at the X20A beam line at the National Synchrotron Light Source. Of great interest here was the asymmetry of the smectic scattering peak and its evolution with temperature and disorder strength. To ensure that the observed effects were due to the sample and not the instrumental resolution, measurements were made at both positive and negative scattering angles. As with previous studies, the number of scans was kept limited to avoid undue radiation damage to the sample. The results obtained in the *N*, Sm*A*, and Sm*C* regimes are reported below.

TABLE I. Characteristics of the aerosil gel structure and the $\bar{8}S5$-aerosil transitions. ρ_S is the mass of aerosil divided by the volume of liquid crystal; Φ is the volume fraction of pores; $\ell_0 = 2/a\rho_S$ is the mean aerosil pore size, where a is the specific silica area [6]; $\xi_\parallel^{NA}$, $\xi_\perp^{NA}$ indicate the approximate Sm*A* parallel and perpendicular correlation lengths close to the *N*-Sm*A* pseudotransition [16]; and T_{AC}^* is the Sm*A*-Sm*C* transition temperature.

ρ_S (g cm^{-3})	Φ	ℓ_0 (Å)	$\xi_\parallel^{NA}$ (Å)	$\xi_\perp^{NA}$ (Å)	T_{AC}^* (K)
0.0	1	∞	∞	∞	329.3±0.1
0.025	0.99	2700	∼40000	∼1000	327.8±0.2
0.039	0.98	1700	∼16000	∼650	323.7±0.4
0.073	0.97	910	∼15000	∼600	323.8±0.2
0.096	0.96	690	8000	340	326.1±0.3
0.220	0.91	300	2400	130	325.9±0.2
0.350	0.86	190	4000	200	327.0±0.2

III. RESULTS AND ANALYSIS

Figure 2 shows a succession of scans of $\bar{8}S5$ with $\rho_S = 0.096$ as the temperature is decreased. At high temperatures in the nematic phase [Fig. 2(a)] there is a broad peak corresponding to short-range pretransitional Sm*A* fluctuations. The observed powder average has a characteristic asymmetry. On reducing the temperature the correlated regions grow in size as indicated by the narrower line profile [Fig. 2(b)]. Unlike bulk $\bar{8}S5$, the liquid crystal enters a Sm*A* state with a finite correlation volume. Further cooling takes the sample toward the Sm*C* state. Prior to the onset of the molecular tilt, the peak begins to broaden [Fig. 2(c)]. As the sample enters the Sm*C* regime the peak moves to higher wave vectors and begins to narrow [Fig. 2(d)]. At the lowest temperatures studied, the angle of molecular tilt exceeds 20° while the line-shape asymmetry is reversed compared to that

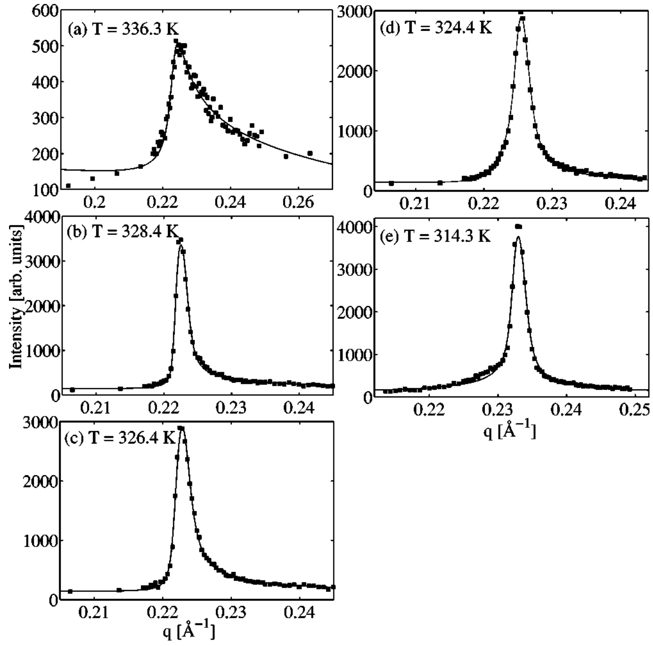

FIG. 2. (a)–(e) The x-ray intensity vs wave-vector transfer with decreasing temperature for a $\overline{8}S5$-aerosil dispersion with $\rho_S = 0.096\ \mathrm{g\,cm^{-3}}$. Panels (a)–(c) show the asymmetric line shape typical of Sm*A* fluctuations in $\overline{8}S5$. The pseudotransition into the short-range Sm*C* state occurs at a temperature just below that for panel (c). The solid lines are the results of fits described in the text.

in the Sm*A* phase [Fig. 2(e)]. The solid lines in Fig. 2 are the results of fits to a model to be described below.

In keeping with previous studies of the *N*-Sm*A* transition in liquid-crystal–aerosil dispersions [3,5], the line shape has been taken to be composed of two terms: the first is based on the line shape for the Sm*A* thermal fluctuations in the pure liquid crystal and the second is the same line shape squared, which corresponds to the contribution of static random-field fluctuations. The latter are caused by the randomly positioned aerosil surfaces pinning the phase of the density wave. The results of fits in Figs. 2(a)–2(c) and in Fig. 3 show that this line shape describes the data in the Sm*A* region very well. The full expression is

$$S_{NA}(\mathbf{q}) = \frac{\sigma_1}{1+\xi_\parallel^2(q_\parallel - q_\parallel^0)^2 + \xi_\perp^2 q_\perp^2 + c\,\xi_\perp^4 q_\perp^4} + \frac{\sigma_2}{[1+\xi_\parallel^2(q_\parallel - q_\parallel^0)^2 + \xi_\perp^2 q_\perp^2 + c\,\xi_\perp^4 q_\perp^4]^2} \qquad (1)$$

which is powder averaged and convoluted with the measured resolution function. In Eq. (1), σ_1 and σ_2 are the amplitudes of the thermal and random-field terms, respectively; $\xi_\parallel$ and $\xi_\perp$ are the correlation lengths parallel and perpendicular to the layer normal; likewise $q_\parallel$ and $q_\perp$ are the components of the wave vector $\mathbf{q}$; $q_\parallel^0$ is the peak position; and c is the coefficient of the fourth-order correction term. The amplitude of the random-field term increases as the temperature is reduced (Fig. 3).

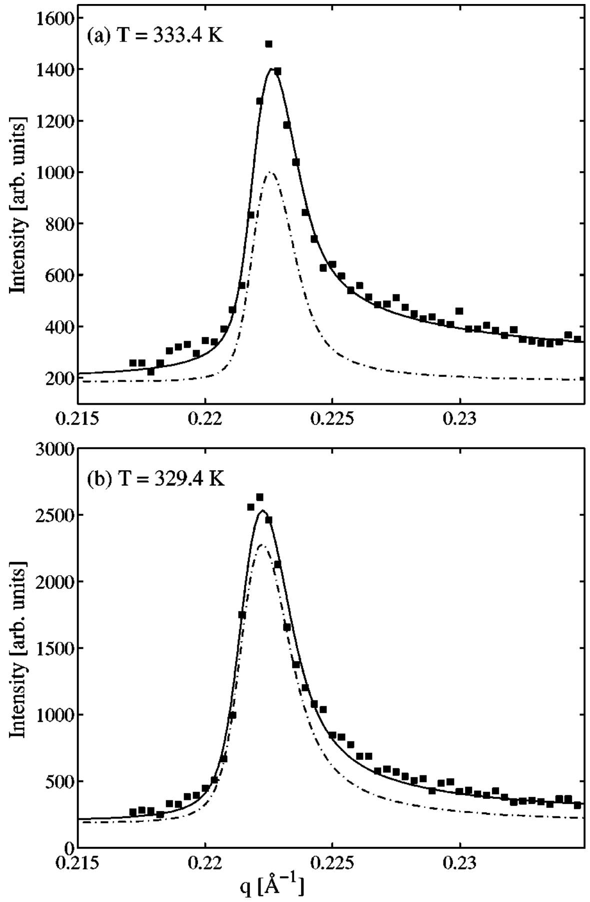

FIG. 3. The x-ray intensity in reciprocal space for a $\overline{8}S5$-aerosil dispersion with $\rho_S = 0.22\ \mathrm{g\,cm^{-3}}$ at two temperatures in the Sm*A* regime. The full line is the result of a fit involving the powder average of Eq. (1) to the data. The broken line represents only the second term corresponding to the random-field fluctuations. The random-field contribution increases with decreasing temperature yielding a characteristic change in the observed line shape.

As with previous studies [2,3,5], it is assumed that the dependence of $\xi_\perp$ and c on $\xi_\parallel$ remains the same in the aerosil samples as it is in the pure materials. It should be noted that the asymmetric line shape is a consequence of powder averaging Eq. (1) for a highly anisotropic correlation volume together with a small value for c in $\overline{8}S5$ which, in turn, means that there are long tails in the transverse direction. This $\overline{8}S5$ line shape cannot be reproduced using the approximation scheme described in Ref. [11] which does not incorporate explicitly the bulk liquid-crystal structure factor. Figure 4 shows the parallel correlation length $\xi_\parallel$ values extracted from the fits. At high temperatures the short-ranged smectic correlations develop in the nematic phase in a similar manner to that in pure $\overline{8}S5$ and to other liquid-crystal–aerosil gels. At temperatures below the bulk *N*-Sm*A* transition temperature the behavior differs from that of the pure material. Estimates of the correlation lengths parallel and perpendicular to the layer normal close to the *N*-Sm*A* pseudotransition [16] are listed for each sample in Table I. The parallel correlation lengths are very much greater than those for 8CB aerosil [2,3] and 8OCB aerosil [5] at the same

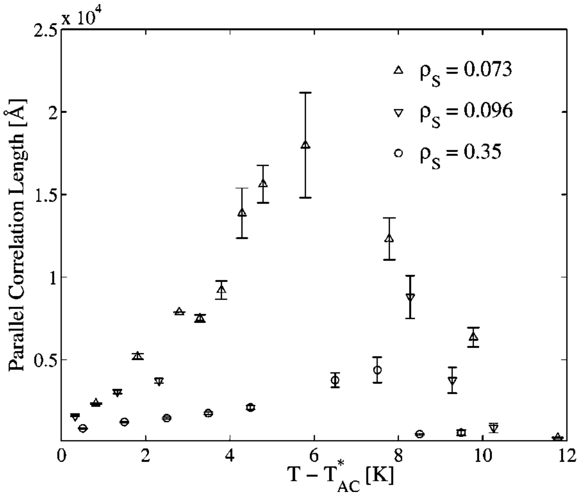

FIG. 4. The parallel correlation length $\xi_\parallel$ for Sm*A* order as a function of temperature as a result of fits of Eq. (1) to the data [15]. The effective transition temperature T^*_{AC} is defined in the text related to Fig. 6, and the values are listed in Table I. Note that for the pure $\overline{8}S5$ material used in this work $T^0_{NA}-T^0_{AC}=7$ K, and the $T_{NA}-T^*_{AC}$ value for all $\overline{8}S5$-aerosil samples is expected to have almost the same value [7].

ρ_S values. These correlation lengths are very long compared to the size of the pores, more than ten times longer for most samples. The highly anisotropic correlation volume is evident from the perpendicular correlation length values. These values are comparatively short, roughly half the mean pore size (Table I). At lower temperatures the behavior in the Sm*A* regime is qualitatively very different from that observed for 8CB-aerosil and 8OCB-aerosil systems [3,5]. The size of the correlated Sm*A* regions in a given $\overline{8}S5$-aerosil sample decreases markedly as the temperature is lowered toward the Sm*A*-Sm*C* transition whereas $\xi_\parallel$ is roughly independent of temperature in the Sm*A* region for the materials with no Sm*C* phase [3,5]. Close to the Sm*A*-Sm*C* transition there is a tilt instability which can be induced by compression and this may make the liquid crystal less resistant to the disordered environment [17].

Figure 5 illustrates the low temperature line shape for the finite range Sm*C* ordered state when $\rho_S=0.073$. The asymmetry is pronounced and is different from that observed when the structure factor has Sm*A* character. The solid line in Fig. 5(a) is the result of a fit of the data to the model given in Eq. (1). This model does not describe the line shape at all well. The solid line in Fig. 5(b) is the result of a fit using the Sm*C* structure factor as the basis for the two-component line shape. The Sm*C* structure factor is taken from studies of the pretransitional *N*-Sm*C* fluctuations in 4-*n*-pentylphenylthiol-4′-*n*-heptyloxybenzoate ($\overline{7}S5$)-$\overline{8}S5$ mixtures, the so called Chen-Lubensky structure factor [18,19]

$$S_{AC}(\mathbf{q})=\frac{\sigma_1}{1+\xi_\parallel^2(q_\parallel-q_\parallel^0)^2-U_pq_\perp^2+V_pq_\perp^4}+\frac{\sigma_2}{[1+\xi_\parallel^2(q_\parallel-q_\parallel^0)^2-U_pq_\perp^2+V_pq_\perp^4]^2}\qquad(2)$$

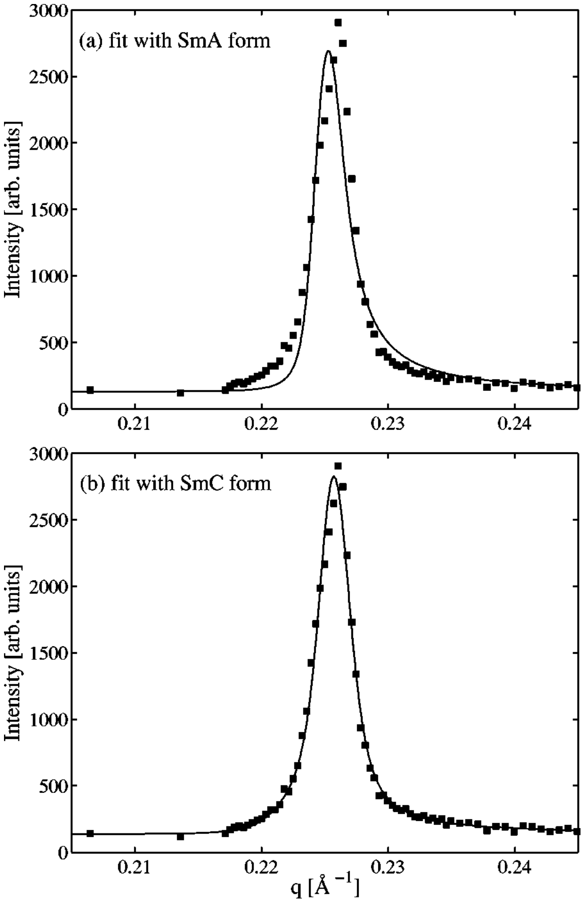

FIG. 5. The line shape for a sample with $\rho_S=0.073\ \mathrm{g\,cm^{-3}}$ at $T=321.5\ \mathrm{K}<T^*_{AC}$. The solid line in (a) shows the result of a fit to a powder average of the Sm*A* form given by Eq. (1) and that in (b) shows the result of a fit to a powder average of the Sm*C* line shape given by Eq. (3).

with $U_p,V_p>0$. This is identical to Eq. (1) except that the coefficient of the $q_\perp^2$ term is assumed to be negative. Since the line shape and the peak position have quite different responses to the porous environment, it is more convenient to restate this structure factor displaying explicitly the component of the peak position perpendicular to the long axis of the molecules, $q_\perp^0$:

$$S_{AC}(\mathbf{q})=\frac{\sigma_1}{1+\xi_\parallel^2(q_\parallel-q_\parallel^0)^2+D_p^2(q_\perp^2-(q_\perp^0)^2)^2}+\frac{\sigma_2}{[1+\xi_\parallel^2(q_\parallel-q_\parallel^0)^2+D_p^2(q_\perp^2-(q_\perp^0)^2)^2]^2}.\qquad(3)$$

This is seen to give a good account of the data in Fig. 5 and Figs. 2(d),2(e). The best fit between this structure factor and the data was found by varying the thermal amplitude σ_1, the random-field amplitude σ_2, the parallel correlation length $\xi_\parallel$, the perpendicular parameter D_p, and the peak position $q_c=\sqrt{[(q_\parallel^0)^2+(q_\perp^0)^2]}=2\pi/d_c$. The two components $q_\parallel^0=q_c\cos\phi$ and $q_\perp^0=q_c\sin\phi$ were determined using the pre-

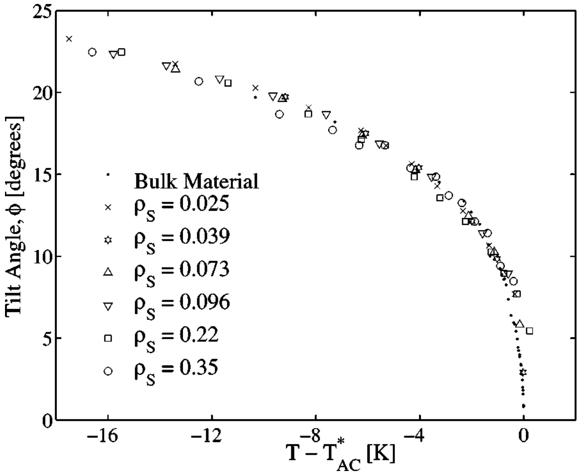

FIG. 6. Temperature dependence (and ρ_S independence) of the molecular tilt angle with respect to the layer normal below T^*_{AC}. The data for bulk $\overline{8}S5$ is taken from Ref. [20]. The values of the effective transition temperatures are given in Table I.

viously determined relationship [20] between the tilt angle ϕ and the layer spacing in the Sm*A* phase, d_a, that is, $\phi = 1.2\sqrt{[2(1-d_c/d_a)]}$.

The Sm*A*-Sm*C* transition in $\overline{8}S5$ is a mean-field transition with the tilt angle as the order parameter [20]. Hence the pretransitional fluctuations are weak in the pure material. Figure 6 shows the tilt angle, as a function of temperature, for the full range of disorder strength studied. The tilt angle was determined from the Sm*C* peak position q_c. The effective transition temperature T^*_{AC} was found by fitting the Landau-Ginzburg tricritical model [13] to the temperature dependence of the tilt angle. When plotted versus $T-T^*_{AC}$, the tilt angles for all samples collapse onto a single curve (Fig. 6). The robustness of ϕ in gels suggests that, while the disorder may be coupling to the position and presumably the orientation of the smectic layers, it is not strongly affecting the molecular orientations [21]. Figure 7 shows parameters extracted from the fits of Eq. (3) to the data acquired below T^*_{AC}. Only results for low ρ_S are presented. In Fig. 7(a) the correlation volume $\xi_\parallel D_p$ is shown as a function of temperature in the Sm*C* region. Increasing the aerosil concentration progressively decreases the extent of the Sm*C* correlations. For higher ρ_S the line shape becomes distorted as will be described below. In Fig. 7(b) the ratio of the random field to thermal amplitudes is presented in the form a_2/σ_1, where $a_2 = \sigma_2/\xi_\parallel D_p$. The ratio a_2/σ_1 is independent of normalization and is predicted to have a power law dependence on ρ_S [4]. Increasing aerosil concentration gives rise to a larger random-field contribution to the structure factor. Note that both Figs. 7(a) and 7(b) show ρ_S dependence for temperatures just below T^*_{AC} that diminishes at lower temperatures. The low temperature behavior could be an early symptom of the distortion that becomes clear for the higher density samples.

Table I lists the Sm*A*-Sm*C* transition temperatures as a function of ρ_S. There is an initial sharp drop followed by a recovery. This effect is not understood, but qualitatively similar variations have been observed at *N*-Sm*A* and *N*-*I* transitions in other liquid-crystal–aerosil gels [6].

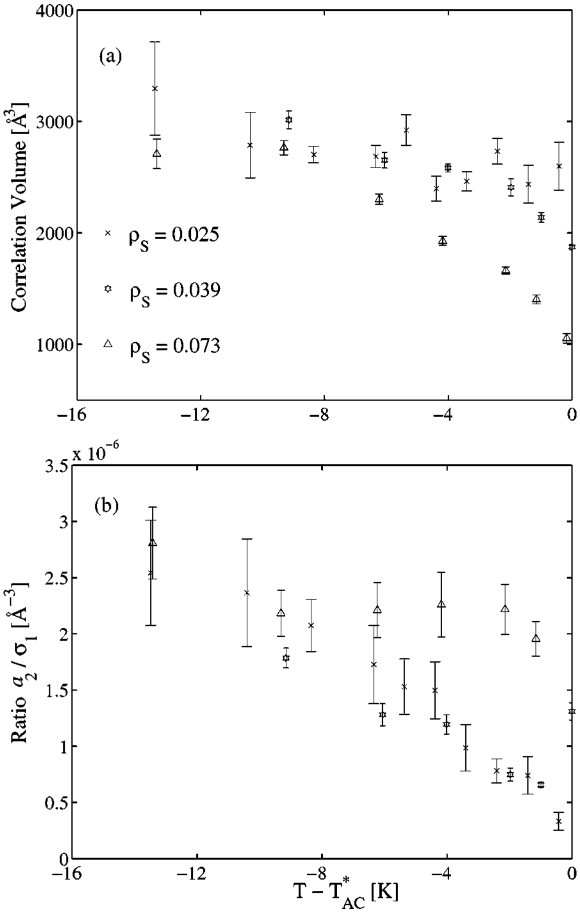

FIG. 7. (a) Correlation volume for Sm*C* order as a function of temperature as a result of fits of Eq. (3) to the data. (b) The ratio of the amplitude of the random-field term, a_2, to the thermal term, σ_1.

For the highest densities of aerosils and the lowest temperatures the peak shape corresponding to Sm*C* fluctuations becomes distorted. A shoulder develops on the low tilt angle side of the reflection peak, as shown in Fig. 8(a). The shoulder becomes more pronounced as the temperature is reduced and as ρ_S is increased. Figure 8(b) shows the result of subtracting the result of a fit [solid line Fig. 8(a)] from the data. A peak is observed which falls between the Sm*A* peak position $q_a = q^0_\parallel$ and the Sm*C* peak position q_c. This behavior indicates that a minority of regions become fixed at lower tilt angles.

IV. CONCLUSIONS

X-ray diffraction results have been presented for $\overline{8}S5$ aerosil dispersions over the temperature range for which the bulk liquid crystal has *N*-Sm*A* and Sm*A*-Sm*C* transitions. The gel of aerosil particles is observed to destroy the Sm*A* and Sm*C* phases in the sense that the ordered states becomes short ranged. Both the short-range order Sm*A* and Sm*C* structure factors are well described by a model assuming random fields. The correct thermal fluctuation structure fac-

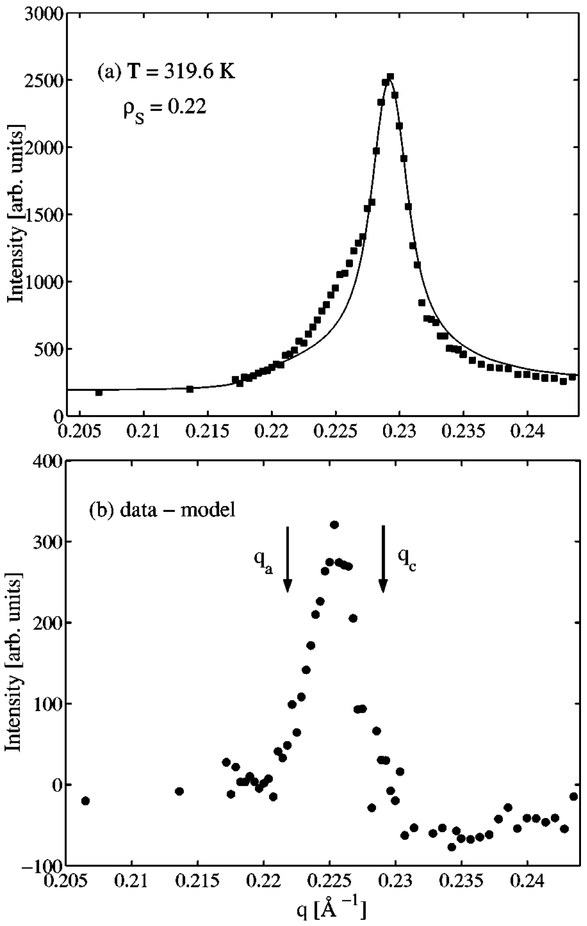

FIG. 8. (a) Distorted line shape in the Sm*C* regime at low temperature and high ρ_S. The solid line is the result of a fit of Eq. (3) to these data. (b) The result of subtracting the fit values from the data points given in part (a). The arrows indicate the positions of the Sm*A*, q_a, and Sm*C*, q_c, peaks, respectively.

tor has to be used as the thermal term and its square as the random-field term. Estimates at low ρ_S and more accurate values for high ρ_S [16] indicate that $\xi_\parallel$, the correlation lengths parallel to the layer normal, are very long compared to those of 8CB and 8OCB for the same pore sizes. This suggests that the nonpolar molecule experiences a weaker pinning field than the polar materials do. The highly anisotropic correlation volume for this material leads to a strong asymmetry in the powder-averaged line shape. This characteristic is consistent with our model and leads to unique values of fit parameters when the best correspondence between Eq. (1) and the data is found. It also makes clear that the two-Lorentzian model used by Bellini and co-workers [11] cannot be applied in this case. That the two-component line shape gives a good account of data for the Sm*A*-Sm*C* transition in $\overline{8}S5$-aerosil gels is intriguing.

For other liquid-crystal–aerosil gels exhibiting *N*-Sm*A* transitions, it has been possible to make detailed comparisons with theoretical models. For 8CB aerosil [2–4] and 8OCB aerosil [5], the parameters extracted from the line shape compared favorably with the predictions of Ref. [22], giving the appearance that the gel applies a random field which pins the phase of the smectic density wave. The low temperature behavior of the correlation length, due to enhanced anomalous elasticity, predicted by Ref. [23] has not been observed for LC-aerosil gels. In $\overline{8}S5$, the Sm*A* regime appears to be strongly affected by the impending Sm*A*-Sm*C* transition. The correlation length is never constant, as for a random-fields model, or increasing on cooling as predicted for anomalous elasticity. Currently there are no theoretical predictions for the effects of a porous random environment on the Sm*A*-Sm*C* transition.

The Sm*A*-Sm*C* tilt (order parameter) behavior is preserved almost unmodified in the aerosil samples. This suggests that any effect that the aerosils may have on the molecular orientations has little consequence for the transition and that this is true even for quite high aerosil concentrations. The bare correlation volume for Sm*A* materials exhibiting a Sm*C* phase can be estimated from the elastic properties of the material and is typically $(70\ \text{Å})^3$ [20]. For the aspect ratio of the $\overline{8}S5$ molecule this is likely to imply a bare correlation length parallel to the molecule of close to ten molecular lengths. This long range of interaction is highly likely to minimize the influence of random disorder. If some small fraction of the molecules are forced to point in uncorrelated random directions they will tend to have no net effect: the large bare correlation length implies an averaging over the disorder. For high ρ_S, the appearance of correlations peaked at a wave vector midway between those of the Sm*A* and Sm*C* phases indicates that small regions of the sample become stuck at a lower tilt angle.

ACKNOWLEDGMENTS

We are grateful to S. LaMarra for technical assistance, to N.A. Clark for discussing unpublished research, and to M. Ramazanoglu for helpful comments. Funding in Toronto was provided by the Natural Science and Engineering Research Council and support was provided at WPI by the NSF under Grant No. DMR-0092786 and at JHU under Grant No. DMR-0134377. Dr Mary E. Neubert and David G. Abdallah, Jr. were supported by NSF grant DMR Grant No. 89-20147.

---

[1] P. G. de Gennes, and J. Prost, *The Physics of Liquid Crystals*, 2nd ed. (Oxford University Press, Oxford, 1993).

[2] S. Park, R.L. Leheny, R.J. Birgeneau, J.-L. Gallani, C.W. Garland, and G.S. Iannacchione, Phys. Rev. E **65**, 050703(R) (2002).

[3] R.L. Leheny, S. Park, R.J. Birgeneau, J.-L. Gallani, C.W. Garland, and G.S. Iannacchione, Phys. Rev. E **67**, 011708 (2003).

[4] G.S. Iannacchione, S. Park, C.W. Garland, R.J. Birgeneau, and R.L. Leheny, Phys. Rev. E **67**, 011709 (2003).

[5] P.S. Clegg, C. Stock, R.J. Birgeneau, C.W. Garland, A. Roshi,

and G.S. Iannacchione, Phys. Rev. E **67**, 021703 (2003).

[6] G.S. Iannacchione, C.W. Garland, J.T. Mang, and T.P. Rieker, Phys. Rev. E **58**, 5966 (1998).

[7] H. Haga and C.W. Garland, Liq. Cryst. **23**, 645 (1997).

[8] C.A. Schantz, and D.L. Johnson, Phys. Rev. A **17**, 1504 (1978).

[9] M.E. Neubert, R.E. Cline, M.J. Zawaski, P.J. Wildman, and A. Ekachai, Mol. Cryst. Liq. Cryst. **76**, 43 (1981).

[10] C. R. Safinya, Ph.D. thesis, Massachusetts Institute of Technology, 1981.

[11] T. Bellini, L. Radzihovsky, J. Toner, and N.A. Clark, Science **294**, 1074 (2001).

[12] C.C. Huang, and J.M. Viner, Phys. Rev. A **25**, 3385 (1982).

[13] R.J. Birgeneau, C.W. Garland, A.R. Kortan, J.D. Litster, M. Meichle, B.M. Ocko, C. Rosenblatt, L.J. Yu, and J. Goodby, Phys. Rev. A **27**, 1251 (1983).

[14] M. Meichle and C.W. Garland, Phys. Rev. A **27**, 2624 (1983).

[15] The parallel correlation lengths for the remaining samples are not presented in this figure for clarity. For low ρ_S, the finite instrumental resolution leads to large error bars and the data points are quite sparse to avoid radiation damage.

[16] All correlation length values listed in Table I were determined by interpolating at a temperature $T = T^*_{AC} + 7$ K (based on the assumption, supported by Ref. [7], that the Sm*A* range has the same value in all aerosil samples as in pure $\overline{8}S5$), and they thus reflect the likely behavior close to the *N*-Sm*A* pseudo-transition. The values for the $\rho_S = 0.025$, 0.039, 0.073 samples are based on fits to the tails of the peak, due to the resolution limited width.

[17] R. Ribotta, R.B. Meyer, and G. Durand, J. Phys. (France) Lett. **35**, L161 (1974).

[18] J-H. Chen, and T.C. Lubensky, Phys. Rev. A **14**, 1202 (1976).

[19] L.J. Martinez-Miranda, A.R. Kortan, and R.J. Birgeneau, Phys. Rev. A **36**, 2372 (1987).

[20] C.R. Safinya, M. Kaplan, J. Als-Nielsen, R.J. Birgeneau, D. Davidov, J.D. Litster, D.L. Johnson, and M.E. Neubert, Phys. Rev. B **21**, 4149 (1980).

[21] The results of fits of the tricritical to mean-field crossover model to the temperature dependence of the tilt angle yields variations in the fit parameters as ρ_S is increased. The fourth-order term in the free energy expansion appears to increase with respect to the second-order term with increasing aerosil concentration. This is consistent with the system moving away from tricriticality. The variation is small and there is no obvious trend in the raw data.

[22] A. Aharony and E. Pytte, Phys. Rev. B **27**, 5872 (1983).

[23] L. Radzihovsky and J. Toner, Phys. Rev. B **60**, 206 (1999).